THE JOURNAL OF BIOLOGICAL CHEMISTRY VOL. 281, NO. 15, pp. 10610–10617, April 14, 2006

Crystal Structure of the V Domain of Human Nectin-like Molecule-1/Syncam3/TsII1/Igsf4b, a Neural Tissue-specific Immunoglobulin-like Cell-Cell Adhesion Molecule*

Received for publication, December 19, 2005, and in revised form, January 12, 2006 Published, JBC Papers in Press, February 7, 2006, DOI 10.1074/jbc.M513459200

Xiuhua Dong[‡§¶], Feng Xu[‡§], Yanhua Gong[¶], Jing Gao[¶], Peng Lin[‡§], Tao Chen[¶], Ying Peng[‡§], Boqin Qiang[¶], Jiangang Yuan[¶], Xiaozhong Peng[¶1], and Zihe Rao[‡§2]

From the [‡]National Laboratory of Biomacromolecules, Institute of Biophysics (IBP), Chinese Academy of Sciences, Beijing 100101, the [§]Tsinghua-IBP Joint Research Group for Structural Biology, Tsinghua University, Beijing 100084, and the [¶]National Laboratory of Medical Molecular Biology, Institute of Basic Medical Sciences, Chinese Academy of Medical Sciences and Peking Union Medical College, National Human Genome Center, Beijing 100005, China

Nectins are Ca^{2+}-independent immunoglobulin (Ig) superfamily proteins that participate in the organization of epithelial and endothelial junctions. Nectins have three Ig-like domains in the extracellular region, and the first one is essential in cell-cell adhesion and plays a central role in the interaction with the envelope glycoprotein D of several viruses. Five Nectin-like molecules (Necl-1 through -5) with similar domain structures to those of Nectins have been identified. Necl-1 is specifically expressed in neural tissue, has Ca^{2+}-independent homophilic and heterophilic cell-cell adhesion activity, and plays an important role in the formation of synapses, axon bundles, and myelinated axons. Here we report the first crystal structure of its N-terminal Ig-like V domain at 2.4 Å, providing insight into *trans*-cellular recognition mediated by Necl-1. The protein crystallized as a dimer, and the dimeric form was confirmed by size-exclusion chromatography and chemical cross-linking experiments, indicating this V domain is sufficient for homophilic interaction. Mutagenesis work demonstrated that Phe^{82} is a key residue for the adhesion activity of Necl-1. A model for homophilic adhesion of Necl-1 at synapses is proposed based on its structure and previous studies.

The cell-cell adhesion systems play important roles in neuronal cell migration, axon-bundle formation, target-cell recognition, activity-dependent plasticity of synapses, and formation of complex glial networks, which surround axons and synapses (1). Nectins are a novel family of Ca^{2+}-independent immunoglobulin-like cell-cell adhesion molecules and comprise four members, termed Nectin-1 to Nectin-4 (2, 3). All Nectins have an extracellular region of three Ig-like domains, a single transmembrane region, and a cytoplasmic tail region (see Fig. 1) (2, 3). Each Nectin forms a homo-*cis*-dimer, in which the monomers are aligned in a parallel orientation, which is then followed by formation of homo-*trans*-dimers in which *cis*-dimers from opposing cell surfaces interact in an anti-parallel orientation, causing cell-cell adhesion (4–8). The first Ig-like domain is necessary and sufficient for the formation of homo-*trans*-dimers, whereas the second Ig-like domain is necessary for the formation of homo-*cis*-dimers (5, 7–9). Furthermore, Nectin-3 can also form a hetero-*trans*-dimer with either Nectin-1 or -2, whereas Nectin-4 also forms a hetero-*trans*-dimer with Nectin-1 (4). The hetero-*trans*-dimers are also mediated by the V domains (9). Nectin-1 has been confirmed to serve as a receptor for all α-herpes viruses tested so far, including herpes simplex virus (HSV)[3] type 1, HSV type 2, and pseudorabies virus, facilitating their entry and cell-cell spread (10, 11). Furthermore, the V domain of Nectin-1 has been demonstrated to play a central role in the interaction with the envelope glycoprotein D of HSV, pseudorabies virus, and bovine herpes virus-1 (12, 13). Therefore, the V domain plays an essential role not only in homophilic and heterophilic *trans*-interactions but also in the process of virion entry (12, 13).

Five molecules with an extracellular region containing three Ig-like domains, one transmembrane region, and one cytoplasmic region have so far been identified and are called Nectin-like molecules (Necls) (Fig. 1) (2). They include Necl-1 (Necl-1/TSLL1/SynCAM3/IGSF4B), Necl-2 (Necl-2/IGSF4/RA175/SgIGSF/TSLC1/SynCAM1) (14–17), Necl-3 (Necl-3/similar to Necl-3/SynCAM2), Necl-4 (TSLL2/SynCAM4), and Necl-5 (Tage4/PVR/CD155) (18). Of these Necls, we focus here on Necl-1/TSLL1/SynCAM3/IGSF4B, from now on referred to as Necl-1. Necl-1 was first sequenced, cloned, and submitted to GenBank™ by our laboratory (accession no. AF062733 (human), in 1998; accession no. AF195662 (mouse), in 1999). *TSLL1* was identified as a *TSLC1*-like gene (19, 20), and SynCAM3 was identified as a member of the SynCAM family (16).

Necl-1 shares Ca^{2+}-independent homophilic and heterophilic cell-cell adhesion activity with Necl-2, Nectin-1, and Nectin-3, but not with Necl-5 or Nectin-2 (21). Unlike the Nectins, Necl-1 does not bind afadin but instead binds membrane-associated guanylate kinase family members (MAGUK) that contain the L27 domain, including Dlg3, Pals2, and CASK (21). RNA blot and *in situ* hybridization analysis showed that Necl-1 is specifically expressed in the nervous system, in a variety of brain regions, including the cortex, cerebellum, hippocampus amygdala, olfactory bulb, and medulla (21). It localizes at the contact sites between two axon terminals, between an axon terminal and an axonal shaft, and between an axon terminal and glia cell processes in the cerebellum. Necl-1 most likely forms homo-*trans*-dimers at these sites (21). In the peripheral myelinated nerve fibers, Necl-1 localizes at the contact

* This work was supported by the 973′ Project (Grants 2001CB510206, 2004CB520801, 2004CB518604, and 2005CB522400) and the Natural Science Foundation of China (Grants 30421003 and 30430200). The costs of publication of this article were defrayed in part by the payment of page charges. This article must therefore be hereby marked "*advertisement*" in accordance with 18 U.S.C. Section 1734 solely to indicate this fact.

The atomic coordinates and structure factors (code 1Z9M) have been deposited in the Protein Data Bank, Research Collaboratory for Structural Bioinformatics, Rutgers University, New Brunswick, NJ (http://www.rcsb.org/).

[1] To whom correspondence may be addressed. Tel.: 86-10-6529-6411; Fax: 86-10-6524-0529; E-mail: pengxiaozhong@pumc.edu.cn.

[2] To whom correspondence may be addressed. Tel.: 86-10-6277-1493; Fax: 86-10-6277-3145; E-mail: raozh@xtal.tsinghua.edu.cn.

[3] The abbreviations used are: HSV, herpes simplex virus; Necl, nectin-like; Ig, immunoglobulin; TSLL1, TSLC1-like; EGS, ethyleneglycol bis-succinimidylsuccinate; MAD, multiple wavelength anomalous dispersion; NCAM, neural cell adhesion molecule; mJAM, murine junctional adhesion molecule; MAGUK, the membrane-associated guanylate kinase; SeMet, seleno-methionyl; JAM1, Junctional adhesion molecule-1.

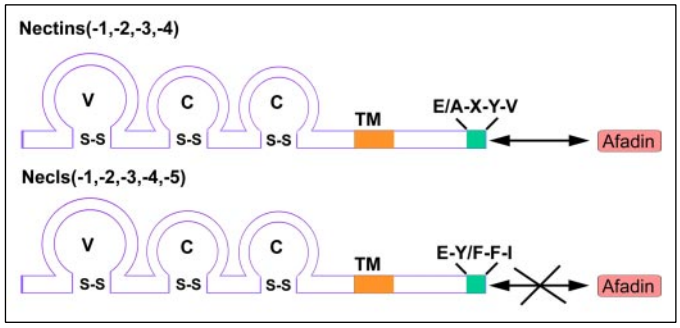

FIGURE 1. **Molecular organization of Necls and Nectins.** The two families share similar structures. They have an extracellular region with three Ig-like domains, a single transmembrane region, and a cytoplasmic tail region. The difference lies in their cytoplasmic region: Nectins can bind to afadin, whereas Necls cannot.

sites between the cellular processes of Schwann cells at the nodes of Ranvier, where it most likely forms homo-*trans*-dimers (21). However, because Necl-1 localizes at the axonal plasma membrane covered with Schwann cell plasma membrane, Necl-1 may form hetero-*trans*-dimers with other cell adhesion molecules, which remain unknown, at these sites (21). To date, no crystal structure has been reported for any portion of any of Necls and Nectins.

To shed more light on the structure and function of Necl-1, we have crystallized the V domain. Here we describe its structure to 2.4-Å resolution and compare it with other known adhesion molecules. The protein was crystallized as a dimer, and a dimeric form was also observed in solution by size-exclusion chromatography and chemical cross-linking experiments, suggesting the first Ig-like domain of Necl-1 is sufficient for the homophilic interaction. A mutation in Phe^{82} disrupted the formation of the dimer, indicating that hydrophobic interactions are very important for dimer formation and suggesting that Phe^{82} may act as a key residue in the adhesion activity of Necl-1. Based on the crystal structure and previous studies, we also propose a V to V model for homophilic adhesion of Necl-1 at synapses. These studies reveal the architecture of this important class of adhesion molecules and provide fundamental insight into *trans*-cellular recognition mediated by Necl-1.

EXPERIMENTAL PROCEDURES

Protein Expression and Purification—The human *necl-1* gene was identified from a large-scale sequencing of human brain. The identification of full-length human *necl-1* cDNA in our laboratory has been described by Zhou and colleagues (22). A fragment containing the coding sequence of Ig-like V domain (corresponding to residues 25–135) was generated by PCR and then cloned into the bacterial expression vector pET32a (Novagen) with a His tag at the N terminus. The recombinant plasmid was transformed into *Escherichia coli* strain BL21(DE3) and overexpressed. Bacterial cells were homogenized by sonication in 1× phosphate-buffered saline (10 mM sodium phosphate, pH 7.4; 150 mM NaCl). The lysates were clarified by centrifugation at 18,000 × *g* for 30 min at 4 °C. The supernatants were then loaded onto a nickel-nitrilotriacetic acid column (Qiagen), equilibrated with 1× phosphate-buffered saline, and then digested with 500 μg of thrombin protease for 16 h at 4 °C. The target protein was washed down and further applied to Resource Q anion-exchange chromatography columns and Superdex-200 size-exclusion (Amersham Biosciences). The purified and concentrated protein (25 mg ml^{-1}) was stored in 20 mM HEPES, pH 7.5, NaCl 100 mM at 193 K. The authenticity of the recombinant Ig-like V domain was confirmed by mass spectroscopy.

The L-SeMet-labeled Ig-like V domain protein was also expressed in *E. coli* strain BL21(DE3). The cells were diluted with adaptive medium (20% LB medium, 80% M9 medium) and grown at 310 K to an A_{600} of 0.6–0.8. The cells were harvested and resuspended in M9 medium, transferred into restrictive medium (1% glucose), and then cultured to an A_{600} of 0.6–0.8 before inducement. L-SeMet at 60 mg $liter^{-1}$; lysine, threonine, and phenylalanine at 100 mg $liter^{-1}$; leucine, isoleucine, and valine at 50 mg $liter^{-1}$; and 0.5 mM isopropyl 1-thio-β-D-galactopyranoside were added, and the incubation continued at 289 K for 20 h. The L-SeMet-labeled Ig-like domain protein was purified and stored under the same condition as the native protein.

A point mutation in one site of interest was introduced by PCR. A mutant of Necl-1 Ig-like V domain (residues 25–135), in which residue Phe^{82} was substituted with Ser, was constructed. The mutant DNA construct was verified by restriction analysis and DNA sequencing. There were no significant variations in expression levels or in purification patterns for the derivative in comparison to wild-type Necl-1 Ig-like V domain (residues 25–135).

Gel-filtration Experiments—The molecular weights of both wild-type and mutant proteins were estimated by gel filtration. All gel-filtration experiments were performed using the same Superdex-200 column (Amersham Biosciences) with the same AKTA explorer system (Amersham Biosciences) under identical conditions, using 25 mM Hepes, pH 7.5, 100 mM NaCl, as an elution buffer, flow rate of 0.5 ml min^{-1}, fraction size of 0.5 ml, sample volume of 1 ml, concentration of protein samples of 5 mg ml^{-1}, and detection by absorbance at 280 nm.

Chemical Cross-linking of the Ig-like V Domain Protein—The gel-filtration purified proteins (including wild-type and mutant proteins) were concentrated to ~2 mg/ml by ultrafiltration (5-kDa cut-off). Proteins were cross-linked with ethylene glycol bis-succinimidylsuccinate (EGS) (Sigma). The reactions were incubated for 2 h on ice at different concentrations of EGS, respectively (0, 0.5, 1.0, 1.5, and 2.0 mM EGS), and quenched with 50 mM glycine. Cross-linked samples were analyzed under reducing conditions by 15% SDS-PAGE.

Crystallization and Data Collection—The protein solutions of Ig-like V domain of Necl-1 and L-SeMet-labeled protein used for crystallization contained 20 mM HEPES, pH 7.5, 100 mM NaCl, and 20 mg ml^{-1} protein. Crystals optimized for x-ray diffraction were obtained using the hanging drop vapor diffusion technique with reservoir solution containing 4 M sodium formate. 1 μl of protein solution was mixed with 1 μl of reservoir solution and equilibrated against 200 μl of reservoir solution at 291 K. The SeMet derivative crystal was grown from the same conditions. Multiwavelength anomalous diffraction (MAD) data for L-SeMet-labeled Ig-like V domain protein were collected using radiation of wavelengths 0.9788, 0.9793, and 0.9700 Å on beamline 3W1A at the Beijing Synchrotron Radiation Facility. The crystal was flash-frozen, and data were collected at 100 K to 2.4-Å resolution using a MAR charge-coupled device detector. Data were indexed and integrated using HKL2000 (23) and scaled and merged using SCALEPACK. The crystal belongs to space group $C222_1$ with unit-cell parameters $a = 77.1$ Å, $b = 77.5$ Å, and $c = 102.2$ Å. The Matthews coefficient suggests the presence of two molecules in an asymmetric unit with an estimated solvent content of 47% (24).

Structure Determination, Refinement, and Analysis—The Ig-like V domain structure was solved by the MAD technique using L-SeMet-labeled protein. The Beijing Synchrotron Radiation Facility data sets were sufficient to solve the phase problem and yielded clear experimental electron density maps. One selenium position was determined, and initial phases were calculated by the program SOLVE (25). Following density modification by RESOLVE (26), the resulting electron density map was of sufficient quality that the entire model, with the exception of several residues at the termini, could be built. The program O (27) was

TABLE 1

Data processing, MAD phasing and refinement statistics

Numbers in parentheses correspond to the highest resolution shell.

Data collection statistics			
Space group	$C222_1$		
Unit cell (Å)	$a = 77.1, b = 77.5, c = 102.2$		
		Se-Met	
Crystal	**Peak**	**Edge**	**Remote**
Wavelength (Å)	0.9788	0.9793	0.9000
Resolution (Å)	50–2.4 (2.49–2.4)	50–2.4 (2.49–2.4)	50–2.4 (2.49–2.4)
Unique reflections	12,352	12,343	12,314
Total reflections	100,961	90,775	97,985
R_{sym} (%)[a]	5.3 (18.9)	5.4 (19.1)	8.2 (35.3)
Completeness (%)	100 (100)	100 (100)	99.9 (98.6)
$\langle I\rangle/\langle\sigma\rangle$	36.4 (9.7)	36.4 (9.3)	19.2 (3.5)
Phasing statistics			
Se atoms found		1 per monomer (total 4)	
Initial phases			
Resolution (Å)		50–2.4	
Figure of merit (FOM)		0.66	
Centric		0.69	
Acentric		0.66	
Refinement statistics			
Resolution (Å)	50–2.4		
No. of reflections in working set	23,098		
No. of protein atoms	1,614		
No. of waters	196		
R_{work}/R_{free} (%)[b]	22.7/27.4		
Average B factors (Å^2)	Chain A	Chain B	
Protein main chain	21.7	22.2	
Protein side chain	24.2	24.8	
Water	29.8		
r.m.s.d. bonds (Å)	0.009		
r.m.s.d. angles (°)	1.6		

[a] $R_{merge} = \Sigma_h\Sigma_i|I_{ih} - \langle I_h\rangle|/\Sigma_h\Sigma_i\langle I_h\rangle$, where $\langle I_h\rangle$ is the mean of the observations I_{ih} of reflection h.
[b] $R_{work} = \Sigma(||F_p(obs)| - |F_p(calc)||)/\Sigma|F_p(obs)|$; R_{free} = R factor for a selected subset (5%) of the reflections that was not included in prior refinement calculations.

used for manual rebuilding of the model, and further refinements by simulated annealing, energy minimization, B factor refinement, and water-picking were performed using crystallography NMR software (CNS) (28).

Sequence alignment was performed using ClustalW (29). Comparison of three-dimensional structures was carried out using the DALI server (30). Structure figures were created using the program MOLSCRIPT (31).

RESULTS

Structure of the Monomer—The structure of the N-terminal domain of Necl-1-(37–141) was solved by the MAD method (Table 1). It contains two β-sheets with a total of nine β-strands (Fig. 2), which classifies it as an Ig-like domain of the variable type (V-set) (32). The nine strands sequentially labeled A (Asp^{43}–Val^{51}), B (Thr^{55}–Asp^{61}), C (Leu^{70}–Ser^{73}), C′ (Leu^{80}–Phe^{82}), C″ (Lys^{85}–Arg^{86}), D (Ile^{93}–Ser^{98}), E (Glu^{102}–Ile^{107}), F (Gly^{116}–Ile^{122}), and G (Arg^{128}–Leu^{137}). A, G, F, C, C′, and C″ form one β-sheet, and B, D, and E form the other β-sheet. All strands are antiparallel, except the A strand and the C-terminal part of the G strand, which are parallel. A cysteine bridge from Cys^{60} to Cys^{120} connects the two sheets. A type II β-turn from Val^{51} to Gly^{54} connects the A strand and the B strand, and two type I β-turns from Asn^{90} to Ile^{93} and Thr^{99} to Glu^{102} connect the C″ and D strands, D and E strands, respectively. The loop between strand C and C′, residues Asp^{74} to Glu^{77}, form a 3_{10} helix. There is a 3_{10} helix (Asp^{39}–Gln^{42}) extended at the N terminus that does not participate in β-sheet formation. Only one salt bridge (Arg^{92}–Asp^{114}) was observed in the monomer. The crystal structure confirms the prediction that Necl-1 belongs to the immunoglobulin superfamily.

Structure of the Dimer and Its Formation—There are two monomers (molecule A and molecule B) in one asymmetric unit with a root mean square deviation of 0.4 Å for the 104 Cα atoms (Fig. 3*A*). Using the program SURFACE (33, 34), we calculate the surface areas buried upon dimer formation as 1405 Å^2 (702.5 Å^2 per monomer). Further analysis revealed that two almost identical clusters of residues are responsible to the majority of the interactions at the dimer interface (Fig. 3*B*). The most prominent feature of the hydrophobic pocket consists of two antiparallel aromatic rings of Phe^{82} from C′ β-strand, and the side chains of Lys^{85} from C″ β-strand of A, B molecules. Five other amino acid residues

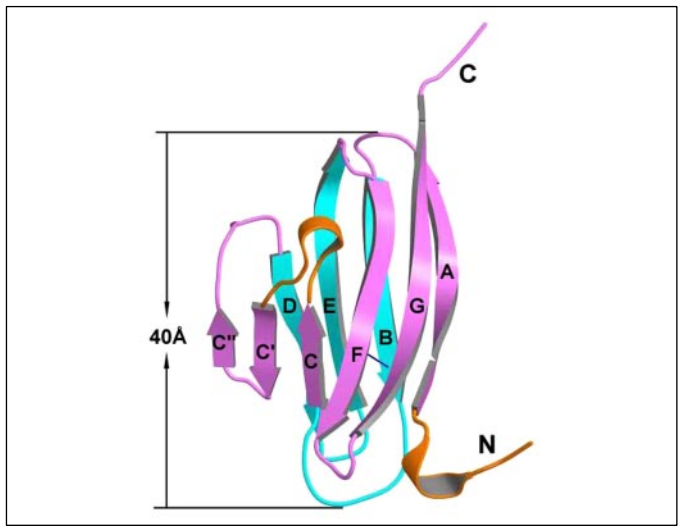

FIGURE 2. **A ribbon drawing of the structure of Necl-1 V domain monomer.** The domain belongs to the V-type subfamily of Ig domains and consists of nine β-strands. The AGFCC′C″ sheet is shown in *pink*, the BDE sheet in *green*, and 3_{10} helices in *orange*. The disulfide bond between strands B and F is in *blue*. The N- and C-terminal are labeled. This figure was prepared using the program MOLSCRIPT.

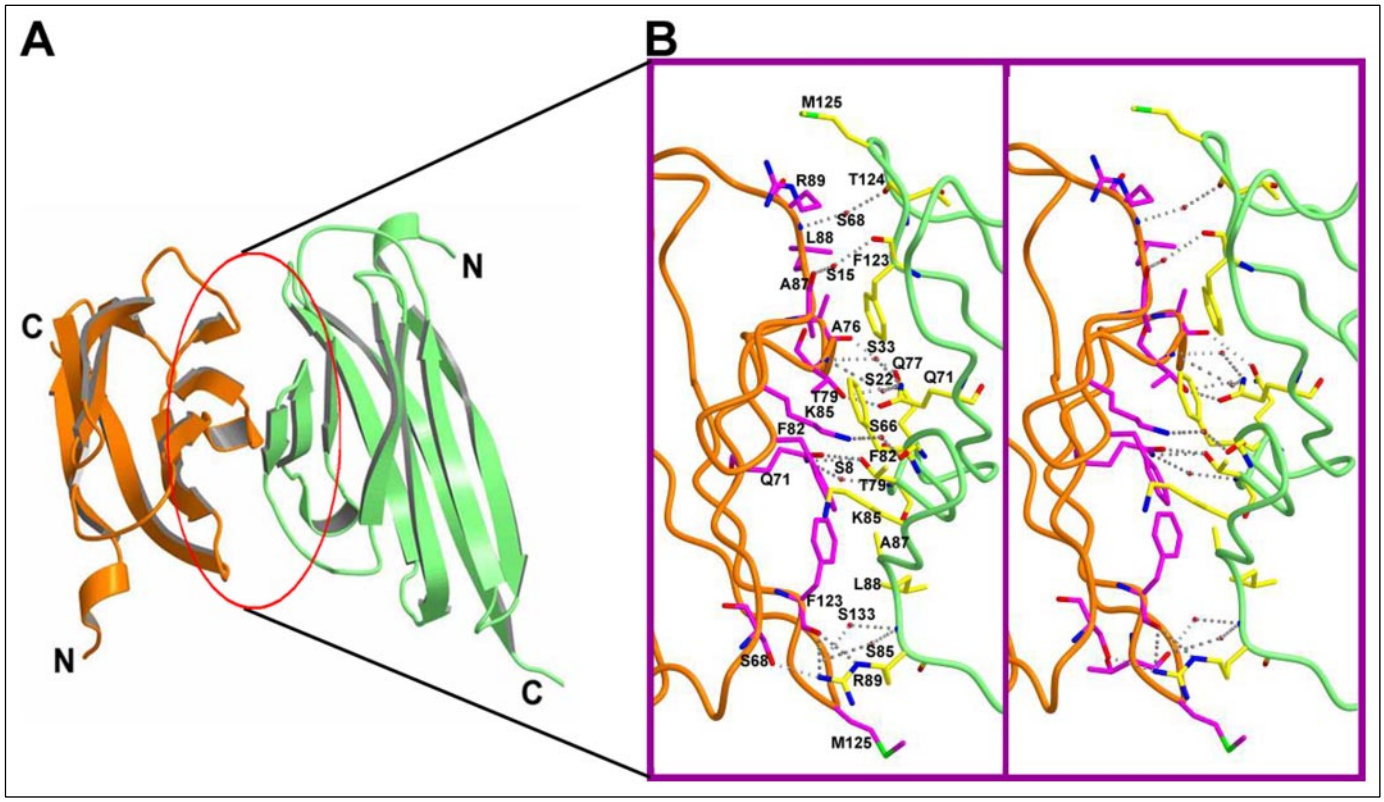

FIGURE 3. **The Necl-1 V homodimer (*A* and *B*).** *A*, a ribbon drawing of the structure of Necl-1 V homodimer, with one monomer shown in *orange* and the other in *green*. *B*, stereo view of the interface between two Necl-1 V monomers. The interface is formed by residues located mainly on C-C′-C″-D β-strands and intervening loops. Residues from one monomer are shown in *pink*, from the other in *yellow*. *Dashed lines* represent hydrogen bonds, and water molecules are shown as *red spheres*. Amino acids are labeled in *single-letter code*.

TABLE 2

Residues involved in dimer formation

The residues involved in hydrophobic interaction are Phe[82], Lys[85], Ala[87], Leu[88], Arg[89], Phe[123], and Met[125].

Direct hydrogen bonds in the A-B interface		
Atom from monomer A	**Atom from monomer B**	**Distance**
		Å
SerA[68] OG	ArgB[89] NH_2	2.75
GlnA[71] OE1	ThrB[79] OG1	2.66
GlnA[71] NE2	ThrB[79] OG1	3.20
ThrA[79] OG1	GlnB[71] OE	2.67
ThrA[79] OG1	GlnB[71] NE2	3.35
AlaA[76] O	GlnB[77] OE1	3.36
PheA[123] O	ArgB[89] NH_2	3.21
PheA[123] O	ArgB[89] NE	3.14

Water-mediated hydrogen bonds				
Atom from monomer A	**Distance**	**Water**	**Distance**	**Atom from monomer B**
	Å		*Å*	
GlnA[71] NE2	2.82	S8	2.84	ThrB[79]N
ThrA[79] N	2.85	S22	2.82	GlnB[71] NE2
ThrA[79] N	2.85	S33	2.82	GlnB[71] NE2
LysA[85] NZ	2.78	S66	2.75	PheB[82] O
AlaA[87] O	2.46	S15	2.74	PheB[123] O
ArgA[89] N	2.77	S68	2.97	ThrB[124] O
ThrA[124] O	2.79	S85	2.94	ArgB[89] N
ThrA[124] O	2.53	S133	2.94	ArgB[89] N

from A and B molecules are also involved in the hydrophobic interaction (Table 2 and Fig. 3*B*). These interactions are supported by eight hydrogen bonds between A and B molecules (Table 2 and Fig. 3*B*). The interaction interface is further stabilized by eight hydrogen bonds via water molecules (Table 2 and Fig. 3*B*). However, no salt bridge was observed in the dimer formation.

Analysis of these amino acid residues found that all these residues involved in dimer interaction are mainly located to the C-C′-C″-D β-strands and intervening loops in Necl1 V domain, except Ser[68] is located in the B–C loop and Phe[123], Thr[124], and Met[125] are located in the F–G loop (Figs. 3 and 4*B*).

Two further experiments demonstrated that the V domain dimer is physiologically relevant: (i) the purified protein elutes at the expected molecular mass for a dimer (~32 kDa) by size-exclusion chromatography (Fig. 5*A*) and (ii) chemical cross-linking further demonstrated that the V domain of Necl-1 forms a dimer (Fig. 5*B*).

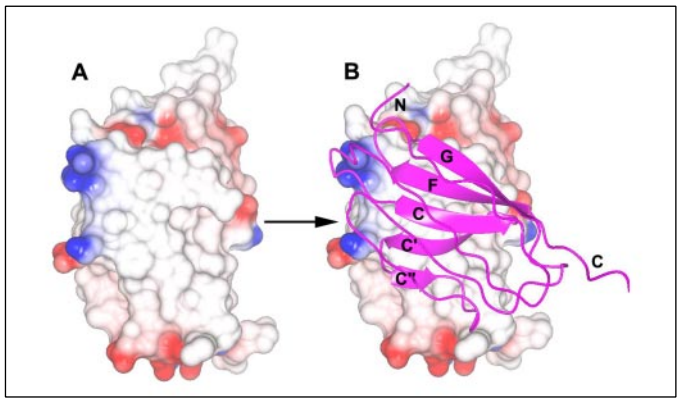

FIGURE 4. *A*, surface representation of the Necl-1 V domain monomer. Hydrophobic residues are shown in *white*, acidic residues in *red*, and basic residues in *blue*. Hydrophobic interactions should be the main force in dimerization. *B*, the homophilic binding interface of Necl-1 V domain. One Necl-1 V monomer is shown in surface representation, and the other is shown as a *pink ribbon*. The interface is formed mainly by C-C′-C″-D β-strands and intervening loops.

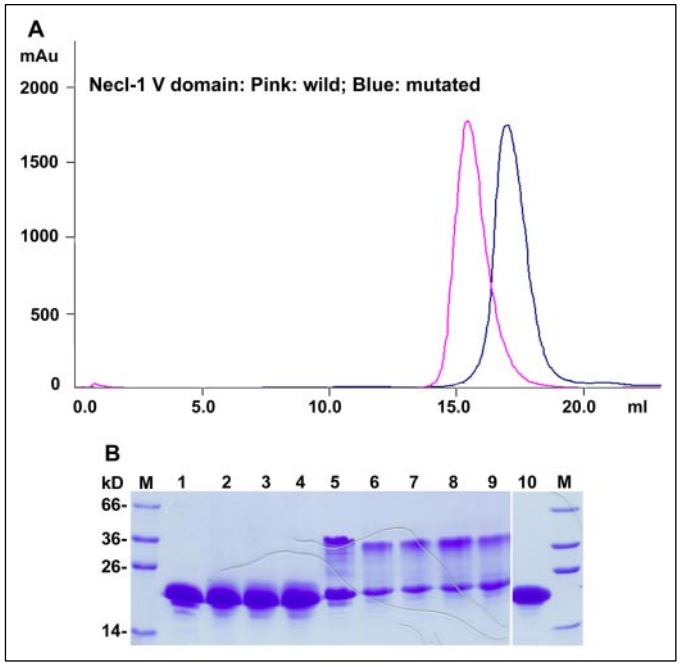

FIGURE 5. *A*, gel-filtration (Superdex200) analysis of the purified wild-type and Phe^{82} → Ser mutant Necl-1 V domain. From the symmetrical peaks of wild (*pink*) and mutated (*blue*) Necl-1 V domain, the Necl-1 V domain most likely forms a dimer. *B*, chemical cross-linking of the wild-type and Phe^{82} → Ser mutant Necl-1 V domain. *Lane M*, molecular mass standards (bands are 66, 36, 26, and 14 kDa, respectively). *Lanes 1–4*, chemical cross-linking of the Phe^{82} → Ser mutant protein. Results are shown with different concentrations of chemical cross-linker, EGS (from Sigma). *Numbers 1–4* indicate the concentrations of the EGS used (0, 0.5, 1.0, and 2.0 mM, respectively). *Lanes 5–9*, chemical cross-linking of the wild-type protein. Results are shown with different concentrations of chemical cross-linker, EGS. *Numbers 5–9* indicate the concentrations of the EGS used (0, 0.5, 1.0, 1.5, and 2.0 mM, respectively). *Lane 10*, the same sample as *lane 5*, also without EGS, but following heat treatment. Only the monomer band was found.

Phe^{82} Is a Key Residue for the Dimerization of the Necl-1 V Domain—Analysis of the dimer suggests that hydrophobic interactions provide the crucial force to maintain the dimer form of the Necl-1 V domain (Fig. 4*A*) and that Phe^{82} should play an important role in the adhesive activity of Necl-1. To test our hypothesis, Phe^{82} was mutated to Ser. When the molecular size of the mutated protein was examined by gel filtration, the protein eluted as a monomer at ~16 kDa. This is in contrast to the wild-type form, which elutes as a dimer at ~32 kDa (Fig. 5*A*). This result was further confirmed by subsequent chemical cross-linking with EGS. From the chemical cross-linking experiments, the dimer bands were clearly seen for the wild-type protein, although a monomer band was also observed. In contrast, no dimer band could be observed for the Phe^{82} → Ser mutant even in high concentrations of cross-linker (Fig. 5*B*). We also observed an interesting phenomenon whereby the wild-type protein could form a dimer even without EGS, but the dimer was completely abolished when the sample was heated (Fig. 5*B*). These results strongly suggest that: (i) the Necl-1 V dimer can exist under physiological conditions; (ii) hydrophobic interactions are the main force to maintain the dimer formation; and (iii) Phe^{82} is a key residue for the dimerization of Necl-1 V domain.

Necls and Nectins May Share Similar Cell-Cell Adhesive Mechanism—There is some disagreement regarding the classification of Necl-5/PVR/CD155 in previous studies. In the review by Takai and colleagues, Necl-5/PVR/CD155 was categorized in the Nectin-like family (2), whereas it was categorized in the Nectin family in other articles (35, 36). However, our phylogenetic analysis showed that Necl-5/PVR/CD155 is closer to the Nectin family than the Nectin-like family (22), but its cytoplasmic tail does not bind to afadin. Therefore, we propose that it may be more rational to re-categorize Necl-5/PVR/CD155 into a new subfamily, which we have tentatively designated Nectin-related molecules, based on their homology to Nectin molecules but inability to bind to afadin (22).

Sequence alignment shows that the full-length Necl-1of human and mouse share 87.3% identity at the amino acid level, and their V domains are almost identical except for the substitution of one Thr by Ser (Fig. 6*A*), which indicates the high conservation of Necl-1 in evolution. The V domains of different Necl-1 to Necl-4 share identities ranging from 36 to 65%. Residues involved in salt bridge formation (Arg^{92}–Asp^{114}) in the monomer are completely conserved. Further analysis indicates that the majority of residues in the dimer interface are highly conserved in the V domains of different Necl members (Fig. 6*B*), which leads to the suggestion that these molecules form similar dimeric structures and may function in a similar way.

Previous studies showed that Nectin-1 forms hetero-*trans*-dimers with Nectin-3 and Nectin-4, and these interactions are mediated through *trans* V to V domain interactions (4, 9). Further studies using chimeric Nectin-1/PVR receptors have shown that the minimal Nectin-3 and Nectin-4 binding region on the Nectin-1 V domain was mapped to the C-C′-C″-D β-strands (5, 37). It may not be mere coincidence that the binding region in Necl-1 V domain is mainly located in the C-C′-C″-D β-strands and intervening loops. These studies suggest that Nectins have a similar structure to Necls, and their extracellular domains mediate cell adhesion by a similar binding mechanism, despite sharing only ~20% identity at the amino acid level. The immunoglobulin family has been demonstrated to share higher homology in structures than in amino acid sequence (32). Thus, the structure of the N-terminal domain of Necl-1 offers a framework for predicting the oligomeric state of other members of the Necl and Nectin family.

Several members of the Nectin and Necl family serve as virus receptors. Human Nectin-1 (poliovirus receptor-related 1 protein) serves as a receptor for all α-herpes viruses. Nectin-2 is also a herpes virus receptor, although for a more restricted set of viruses, and Necl-5 was originally identified as the poliovirus receptor (4, 5). It has been shown using chimeric Nectin-1/poliovirus receptor molecules that the first N-terminal V-type domain of human Nectin-1 mediates virus entry into cells and also binds glycoprotein D, whereas the HSV entry activity mapped entirely to the human Nectin-1 portion located between residues 64 and 94, a region likely to encode the C, C′, and C″ β-strands and intervening loops (23). In our structure, the binding region in the V domain of Necl-1 was also

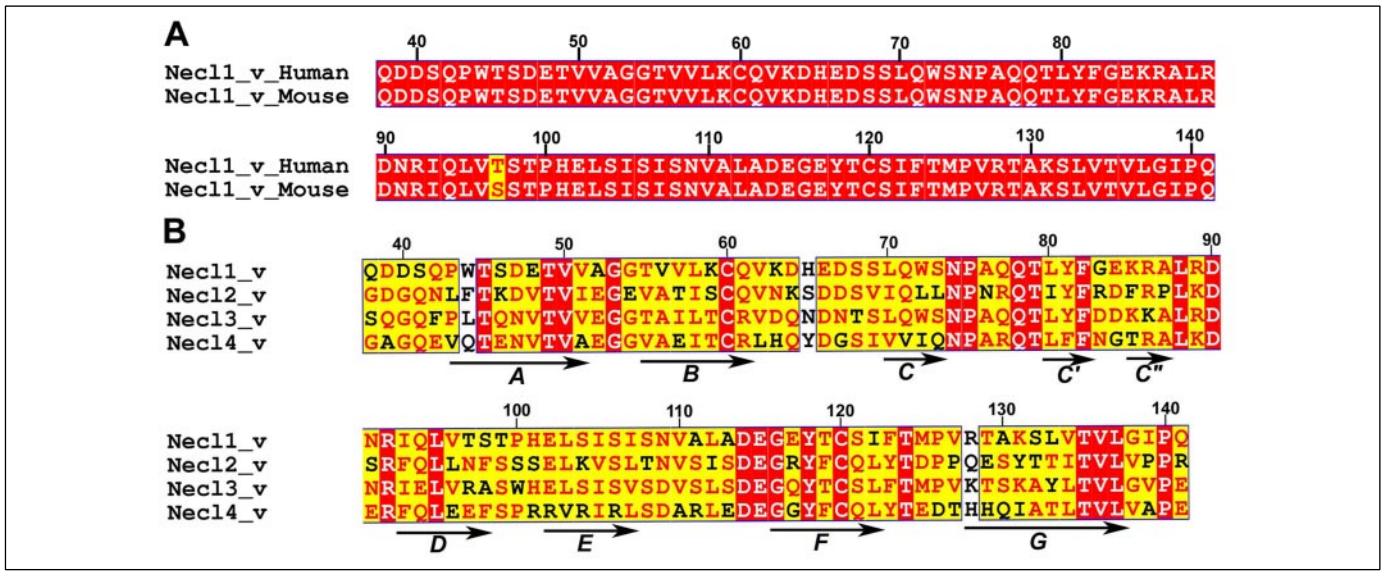

FIGURE 6. **Sequence alignment.** Residues conserved in all sequences are shown in *red*. *Arrows* indicate β-strands, and *numbers* above indicate the position of residues in the structure. *A*, comparison of the sequences of the human Necl-1 V domain with the mouse Necl-1 V domain. *B*, comparison of the sequences of the V domain of Necl-1 with the equivalent domains of Necl-2, -3, and -4.

mainly located to the C-C′-C″-D β-strands and intervening loops. No experiments have so far been reported to confirm that Necl-1 serves as a virus receptor; if it were the case, the virus binding region would possibly be located in the C-C′-C″-D β-strands and intervening loops. Therefore, the structure of the first N-terminal domain may provide a mechanism for virus binding to Nectins and Necls.

Comparison with Other Adhesion Molecule Structures—Comparison of three-dimensional structures was carried out using the DALI server (30). A structural alignment for the Necl-1 V domain was constructed manually by superposition of three-dimensional structures (with high scoring molecules) and correlation of related sequences. Although several overall structures of proteins are similar to the Necl-1 V domain, it was most homologous to one known domain structure in one molecule and to a different domain structure in another molecule. Because the Necl-1 V domain shares a relatively high degree of homology to the D1 domains of NCAM (PDB ID: 2NCM) and mJAM1 (PDB ID: 1F97-A), the Cα atoms of these three adhesion molecules were superimposed to analyze their structural similarities (see Fig. 8). The three proteins all belong to Ca^{2+}-independent Ig superfamily.

NCAM is a glycoprotein expressed on the surface of most cells in the central and peripheral nervous systems, it plays a key role during development and regeneration of the nervous system, and is involved in synaptic plasticity associated with memory and learning (38, 39). NCAM D1 lacks the C″ strand, which classifies it as an intermediate type (I-set) Ig-like domain (38) (Fig. 7). It may not be mere coincidence that the closest available homologous structure to V domain of Necl-1 is the NCAM D1 domain, because the presence of both Necl-1 and NCAM in central and peripheral nervous systems may indicate a recent evolution from a common precursor. The biological function of Necl-1 is not clear; however, available evidence suggests that it localizes at the contact sites of axons, their terminals, and glia cell processes that cooperatively form synapses, axon bundles, and myelinated axons.

Junctional adhesion molecule-1 (JAM1) is an Ig superfamily protein with two Ig-like domains in its extracellular region; it plays a role in the formation of endothelial and epithelial tight junction and serves as a receptor for reovirus (40). Although both JAM1 D1 and Necl-1 V domains belong to the same Ig-like V-set type, there are several differences, and their structures can be superimposed with a root mean square deviation of 4.7 Å for 100 Cα atoms. The strands C and C′ in the JAM1 D1 domain are much longer than those in Necl-1, and its strand C″ is not typical. The D and E strands in JAM D1 are much shorter than those in the Necl-1 V domain due to the lack of five residues in this part (Fig. 7). From the above analysis, we can see that the biggest difference among Necl-1, NCAM, and JAM1 D1 domains lies in their C-C′- C″-D β-strands, which may partly account for their different binding mechanisms in cell adhesion.

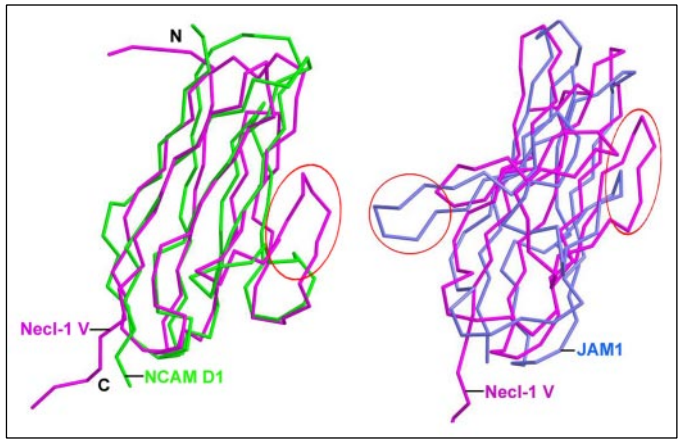

FIGURE 7. **Comparison between the V domain of Necl-1 with the D1 domains of NCAM, JAM1.** *Pink*, Necl-1 V; *green*, NCAM D1; *blue*, JAM1 D1. The difference between three structures mainly lies in the region of the C-C′-C″-D β-strands and intervening loops.

Recently, a novel structural motif, R(V/I/L/)E, has been described in the D1 domain of the three known JAM1, -2, and -3 members, which was shown to be essential for the *cis*-dimerization of the molecule (40). Interestingly, this consensus motif is also present between the C″ and D β-strands in the V domain of Necl-3 (residues 88–90), Necl-4 (residues 95–97), Necl-5 (residues 114–116), Nectin-1 (residues 96–98), and Nectin-4 (residues 120–122) but is absent from Necl-1. Additional experiments will be necessary to study whether this motif plays a role in the adhesive activity of Necls and Nectins.

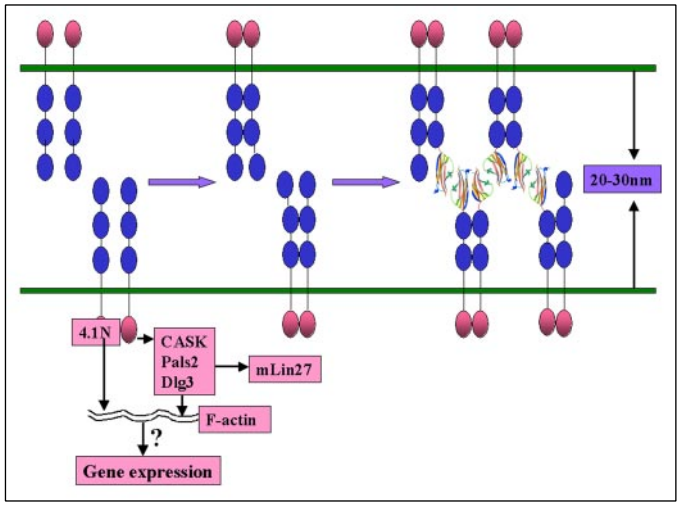

FIGURE 8. **Schematic representation of the proposed mechanism of homophilic adhesion mediated by Necl-1 at synapses, based on the crystal structure.** The cell surfaces are shown in *green* with Necl-1 protruding from them. The Necl-1 monomers, shown on the *left*, first form *cis*-dimers, and then form *trans*-dimers, eventually causing cell-cell adhesion (shown on the *right*).

DISCUSSION

A Model for Homophilic Adhesion of Necl-1 at Synapses—Tissue distribution analysis showed that Necl-1 is specifically expressed not only in the central nervous system but also in the peripheral nervous system. Immunofluorescence and immunoelectron microscopy revealed that Necl-1 localized at the contact sites of axons, their terminals, and glia cell processes that cooperatively form synapses, axon bundles, and myelinated axons. In peripheral myelinated nerve fibers, Necl-1 was localized at the contact sites of the cellular processes of Schwann at the nodes of Ranvier. At these locations, Necl-1 showed Ca^{2+}-independent homophilic and heterophilic cell-cell adhesion activity with Necl-2, Nectin-1, and Nectin-3 but not with Necl-5 or Nectin-2 (21).

Previous studies on Nectins showed that each Nectin first forms *cis*-dimers, then forms *trans*-dimers, eventually causing cell-cell adhesion (4–8). In the structure of the Necl-1 V domain, two monomers should be antiparallel, although there is still an angle between them, which shows that the dimer should be a *trans*-dimer. Combining all available evidence, we propose a model for Necl-1 interactions at synapses. Similar to the mode of action of Nectins, it is likely that Necl-1 first forms *cis*-dimers through the second Ig-like loop, and then forms *trans*-dimers through the first Ig-like loop, eventually causing neural cell adhesion. If we repeat this structural motif of two dimers over several neighboring unit cells, we obtain a two-dimensional molecular network in which the N-terminal V domains contact each other in a common central plane. The C-terminal domains extend almost perpendicular from either side of that plane, as if they were emanating from opposing cell surfaces (Fig. 8).

The structure of the Necl-1 V domain also provides evidence that the *trans*-interaction between Necl-1 is mediated through direct V to V Ig-like domain interactions. We estimate the V domain to be ~40 Å in length (Fig. 2), so the V to V domain interaction is compatible with the size of the intercellular space at synapses, which has been evaluated to be 20–30 nm. Thus, it is reasonable from a structural basis that Necl-1 localizes and mediates cell-cell adhesion at synapses. The V to V model of Necl-1 *trans*-homodimer interactions could probably be extended to Necl-1 *trans*-heterodimer interactions with Necl-2 and Nectin-1 because of their similar domain structures.

The C-terminal cytoplasmic region of Necl-1 does not bind afadin but instead binds members of the MAGUK subfamily that contain the L27 domain, including Dlg3, Pals2, and CASK (21). Zhou and colleagues (22) also demonstrated that Necl-1 can recruit protein 4.1N to the plasma membranes through its C terminus. By associating with the F-actin cytoskeleton though proteins Dlg3, Pals2, CASK, and 4.1N, Necl-1 may play important roles in synaptic architecture and function and is involved in the morphological development, stability, and dynamic plasticity of the nervous system (22, 41). Thus, the homodimer interaction of Necl-1 and its heterodimer interactions with other molecules may not only lead to cell-cell adhesion but also play a role in signal transduction in neural systems.

Acknowledgments—We are grateful to Dr. Mark Bartlam, Yujia Zhai, and Fei Sun for fruitful discussion and technical assistance and Zhiyong Lou, Sheng Ye, Ping Sun, and Qiang Zhao for their valuable help.

REFERENCES

1. Redies, C., and Takeichi, M. (1996) *Dev. Biol.* **180,** 413–423
2. Takai, Y., Irie, K., Shimizu, K., Sakisaka, T., and Ikeda, W. (2003) *Cancer Sci.* **94,** 655–667
3. Takai, Y., and Nakanishi, H. (2003) *J. Cell Sci.* **116,** 17–27
4. Satoh-Horikawa, K., Nakanishi, H., Takahashi, K., Miyahara, M., Nishimura, M., Tachibana, K., Mizoguchi, A., and Takai, Y. (2000) *J. Biol. Chem.* **275,** 10291–10299
5. Reymond, N., Fabre, S., Lecocq, E., Adelaide, J., Dubreuil, P., and Lopez, M. (2001) *J. Biol. Chem.* **276,** 43205–43215
6. Lopez, M., Aoubala, M., Jordier, F., Isnardon, D., Gomez, S., and Dubreuil, P. (1998) *Blood* **92,** 4602–4611
7. Miyahara, M., Nakanishi, H., Takahashi, K., Satoh-Horikawa, K., Tachibana, K., and Takai, Y. (2000) *J. Biol. Chem.* **275,** 613–618
8. Momose, Y., Honda, T., Inagaki, M., Shimizu, K., Irie, K., Nakanishi, H., and Takai, Y. (2002) *Biochem. Biophys. Res. Commun.* **293,** 45–49
9. Fabre, S., Reymond, N., Cocchi, F., Menotti, L., Dubreuil, P., Campadelli-Fiume, G., and Lopez, M. (2002) *J. Biol. Chem.* **277,** 27006–27013
10. Campadelli-Fiume, G., Cocchi, F., Menotti, L., and Lopez, M. (2000) *Rev. Med. Virol.* **10,** 305–319
11. Spear, P. G., Eisenberg, R. J., and Cohen, G. H. (2000) *Virology* **275,** 1–8
12. Cocchi, F., Lopez, M., Menotti, L., Aoubala, M., Dubreuil, P., and Campadelli-Fiume, G. (1998) *Proc. Natl. Acad. Sci. U. S. A.* **95,** 15700–15705
13. Krummenacher, C., Rux, A. H., Whitbeck, J. C., Ponce-de-Leon, M., Lou, H., Baribaud, I., Hou, W., Zou, C., Geraghty, R. J., Spear, P. G., Eisenberg, R. J., and Cohen, G. H. (1999) *J. Virol.* **73,** 8127–8137
14. Urase, K., Soyama, A., Fujita, E., and Momoi, T. (2001) *Neuroreport* **12,** 3217–3221
15. Wakayama, T., Ohashi, K., Mizuno, K., and Iseki, S. (2001) *Mol. Reprod. Dev.* **60,** 158–164
16. Biederer, T., Sara, Y., Mozhayeva, M., Atasoy, D., Liu, X., Kavalali, E. T., and Sudhof, T. C. (2002) *Science* **297,** 1525–1531
17. Yageta, M., Kuramochi, M., Masuda, M., Fukami, T., Fukuhara, H., Maruyama, T., Shibuya, M., and Murakami, Y. (2002) *Cancer Res.* **62,** 5129–5133
18. Ikeda, W., Kakunaga, S., Itoh, S., Shingai, T., Takekuni, K., Satoh, K., Inoue, Y., Hamaguchi, A., Morimoto, K., Takeuchi, M., Imai, T., and Takai, Y. (2003) *J. Biol. Chem.* **278,** 28167–28172
19. Fukuhara, H., Kuramochi, M., Nobukuni, T., Fukami, T., Saino, M., Maruyama, T., Nomura, S., Sekiya, T., and Murakami, Y. (2001) *Oncogene* **20,** 5401–5407
20. Fukami, T., Satoh, H., Williams, Y. N., Masuda, M., Fukuhara, H., Maruyama, T., Yageta, M., Kuramochi, M., Takamoto, S., and Murakami, Y. (2003) *Gene* **323,** 11–18
21. Kakunaga, S., Ikeda, W., Itoh, S., Deguchi-Tawarada, M., Ohtsuka, T., Mizoguchi, A., and Takai, Y. (2005) *J. Cell Sci.* **118,** 1267–1277
22. Zhou, Y., Du, G., Hu, X., Yu, S., Liu, Y., Xu, Y., Huang, X., Liu, J., Yin, B., Fan, M., Peng, X., Qiang, B., and Yuan, J. (2005) *Biochim. Biophys. Acta* **1669,** 142–154
23. Otwinowski, Z., and Minor, W. (1997) in *Macromolecular Crystallography, part A* (Carter, C. W., Jr., and Sweet, R. M., eds) pp. 307–326, Academic Press, New York
24. Matthews, B. W. (1968) *J. Mol. Biol.* **33,** 491–497
25. Terwilliger, T. C., and Berendzen, J. (1999) *Acta Crystallogr. Sect. D* **55,** 849–861
26. Terwilliger, T. C. (2000) *Acta Crystallogr. Sect. D* **56,** 965–972
27. Jones, T. A., Zou, J. Y., Cowan, S. W., and Kjeldgaard, M. (1991) *Acta Crystallogr. Sect. A* **47,** 110–119
28. Brunger, A. T., Adams, P. D., Clore, G. M., DeLano, W. L., Gros, P., Grosse-Kunstleve,

R. W., Jiang, J. S., Kuszewski, J., Nilges, M., Pannu, N. S., Read, R. J., Rice, L. M., Simonson, T., and Warren, G. L. (1998) *Acta Crystallogr. Sect. D* **54,** 905–921
29. Thompson, J. D., Higgins, D. G., and Gibson, T. J. (1994) *Nucleic Acids Res.* **22,** 4673–4680
30. Holm, L., and Sander, C. (1998) *Nucleic Acids Res.* **26,** 316–319
31. Kraulis, P. J. (1991) *J. Appl. Crystallogr.* **24,** 946–950
32. Bork, P., Holm, L., and Sander, C. (1994) *J. Mol. Biol.* **242,** 309–320
33. Lee, B., and Richards, F. M. (1971) *J. Mol. Biol.* **55,** 379–400
34. Chothia, C. (1975) *Nature* **254,** 304–308
35. Reymond, N., Imbert, A. M., Devilard, E., Fabre, S., Chabannon, C., Xerri, L., Farnarier, C., Cantoni, C., Bottino, C., Moretta, A., Dubreuil, P., and Lopez, M. (2004) *J. Exp. Med.* **199,** 1331–1341
36. Fabre-Lafay, S., Garrido-Urbani, S., Reymond, N., Goncalves, A., Dubreuil, P., and Lopez, M. (2005) *J. Biol. Chem.* **280,** 19543–19550
37. Cocchi, F., Lopez, M., Dubreuil, P., Campadelli Fiume, G., and Menotti, L. (2001) *J. Virol.* **75,** 7987–7994
38. Thomsen, N. K., Soroka, V., Jensen, P. H., Berezin, V., Kiselyov, V. V., Bock, E., and Poulsen, F. M. (1996) *Nat. Struct. Biol.* **3,** 581–585
39. Kasper, C., Rasmussen, H., Kastrup, J. S., Ikemizu, S., Jones, E. Y., Berezin, V., Bock, E., and Larsen, I. K. (2000) *Nat. Struct. Biol.* **7,** 389–393
40. Kostrewa, D., Brockhaus, M., D'Arcy, A., Dale, G. E., Nelboeck, P., Schmid, G., Mueller, F., Bazzoni, G., Dejana, E., Bartfai, T., Winkler, F. K., and Hennig, M. (2001) *EMBO J.* **20,** 4391–4398
41. Biederer, T., and Sudhof, T. C. (2001) *J. Biol. Chem.* **276,** 47869–47876